Amperometric proton selective sensors utilizing ion transfer reactions across a microhole liquid/gel interface†‡

Shaikh Nayeem Faisal,[a] Carlos M. Pereira,[b] Sangchul Rho[c] and Hye Jin Lee*[a]

Received 31st May 2010, Accepted 21st July 2010
DOI: 10.1039/c0cp00750a

A new cost-effective amperometric proton selective sensor utilizing a single microhole interface between two immiscible electrolyte solutions (ITIES) is developed. The sensing methodology is based on measuring currents associated with proton transfer across the interface assisted by a proton selective ionophore. The ellipse shaped micro-interface was first fabricated by simple mechanical punching with a sharp needle on a thin PVC film (12 μm thick) commercially available as a food wrapping material. The microhole was then filled up with a gellified polyvinylchloride (PVC)-2-nitrophenyloctylether (NPOE) to create a single microhole liquid/liquid interface. Direct ion transfer reactions across the polarized interface serving as ion sensing platforms were studied using cyclic voltammetry. In order to enhance the selectivity of proton sensing, a proton selective ionophore, octadecyl isonicotinate (ETH1778), was incorporated into the organic gel layer and their electrochemical sensing characteristics were investigated using cyclic voltammetry and differential pulse stripping voltammetry. As an example, we employed the proton selective sensor for the determination of glucose concentrations. The detection scheme involves two steps: (i) protons are first generated by the oxidation of glucose with glucose oxidase in the aqueous phase; and (ii) the current associated with the proton transfer across the interface is then measured for correlating the concentration of glucose.

I. Introduction

Ion transfer reactions across the interface between two immiscible electrolyte solutions (ITIES) have provided a promising sensing platform. The current associated with ion transfer processes across the ITIES increases proportionally as a function of the concentration of target ionic species.[1–3] The other major advantage of using this type of an amperometric ion selective sensor is that the selectivity and sensitivity of the sensor could be controlled by incorporating target specific ionophores in the organic electrolyte to assist the transfer of target ionic species. Extensive efforts have been made to develop the ITIES as more convenient sensing platform by reducing the complexity of handling two liquids. This has been usually obtained by miniaturizing the interface as well as gellifying one of the phases.[4–6] For example, an array of microhole interfaces was fabricated using UV-laser photoablation on polymer film (especially on polyethylene terephthalate film) followed by filling up each hole with gellified organic phase, called ionodes. This provides an excellent way to minimize the Ohmic drop across the interface *via* the use of a smaller interface and to enhance greatly the ion sensing signal due to the use of a well-defined array of microholes where each hole acts as an individual micro-ITIES. Alternatively, microporous silicon membrane fabricated by wet and dry etch techniques could also be utilized as micro-interfaces for ion sensing.[7] Other efforts also include the use of hydrophobic ionic liquids as an alternative organic phase containing supporting electrolyte.[8,9]

The micro-ITIES has found powerful applications in the detection of various ionic species including heavy metal and alkali metal ions, drugs and biomolecules. In particular, great improvements in the detection of hydrophilic ionic species including protons, alkali metal, heavy metal and other ions have been achieved by incorporating ionophores in one of the phases which selectively interact with the ions of interest.[10–12] The role of ionophores usually lowers the apparent Gibbs energy of transfer of ions by assisting their transfer reactions within the potential window. For instance, assisted transfer of Cd(II) ions by ETH 1062 across ionodes fabricated in a strip sensing platform was developed for the ultra-sensitive and selective detection of Cd(II) ions present in an aqueous phase.[13] In addition, the detection of oligopeptides, proteins and a synthetic heparin mimetic based on their transfer process across the ITIES has been extensively investigated.[14–16] Besides the direct detection of dissociated charged species, indirect detection of neutral molecules by monitoring their charged species produced from the subsequent enzymatic reactions has gained great interest from biosensor researchers.[17,18] For example, the transfer process across the ITIES of protons generated by the glucose oxidase reaction *via* oxidizing

[a] *Department of Chemistry, Kyungpook National University, 1370 Sankyuk-dong, Buk-gu, Daegu-city, 702-701, Republic of Korea. E-mail: hyejinlee@knu.ac.kr*
[b] *Centro de Investigação em Química—UP, L4, Departamento de Química da Faculdade de Ciências, Universidade do Porto, Rua do Campo Alegre, 687, 4169-007 Porto, Portugal*
[c] *THE BIO R&D center, THEBIO Co., Ltd, 208 Pohang Technopark, 601, Jigok-dong, Nam-gu, Pohang, Gyeongbuk, 790-834, Republic of Korea*

† Electronic supplementary information (ESI) available: SEM image showing a single microhole filled with PVC-NPOE gel. See DOI: 10.1039/c0cp00750a

‡ Contributed to the *PCCP* collection on Electrified Surface Chemistry, following the 1st Ertl Symposium on Electrochemistry and Catalysis, 11–14 April, 2010, Gwangju, South Korea.

glucose could provide a great alternative for creating glucose biosensors.[19] The facilitated transfer of protons by phospholipid interfacial films at the interface has also been applied as a model of biological membranes to elucidate chemical energy generation in living systems.[20]

In this paper, we describe a simple and cost-effective amperometric proton selective sensor using a single microhole-ITIES fabricated by mechanical punching of the hole with a sharp needle on a thin PVC film (12 μm thick) commercially available as a food wrapping material. The microhole was filled up with a gellified polyvinylchloride-2-nitrophenyloctylether (PVC-NPOE) to create a more convenient sensing platform. Direct ion transfer reactions across the polarized microhole interface were first characterized using cyclic voltammetry. In order to selectively detect protons, we incorporated a proton selective ionophore, octadecyl isonicotinate (ETH1778) into the PVC-NPOE gel layer. The assisted proton transfer by ETH1778 was then investigated using cyclic voltammetry and differential pulse stripping voltammetry. Confirming the reproducible and robust responses for proton sensing, the sensor was finally applied to glucose sensing by means of measuring protons transferring across the microhole interface formed due to the oxidation of glucose with glucose oxidase in the aqueous phase.

II. Experimental

Chemicals

Polyvinylchloride (PVC, high molecular weight, Sigma-Aldrich), *o*-nitrophenyloctylether (NPOE, Fluka), hydrochloric acid (HCl 37%, Merck), octadecyl isonicotinate (ETH1778, Fluka), tetramethylammonium chloride (TMACl, >97%, Sigma-Aldrich), D-(+)-glucose monohydrate ($C_6H_{12}O_6$, Sigma-Aldrich), glucose oxidase from *Aspergillus niger* (200 unit/mg, Fluka), tetrabutylammonium chloride (TBACl, Aldrich), bis(triphenylphosphoranylidene)ammonium chloride (BTPPACl, Fluka) sodium chloride (NaCl, Merck) and lithium chloride (LiCl, Fluka) were all used as received. The supporting electrolytes for the organic phase were bis(triphenyl-phosphoranylidene) ammonium tetrakis(4-chlorophenyl)borate (BTPPATPBCl) or tetrabutylammonium tetrakis (4-chloro-phenyl) borate (TBATPBCl) prepared as described in the previous paper.[5,21] Millipore-filtered water was used for preparing all aqueous solutions.

Fabrication of single microhole-ITIES

A 12 μm thick PVC film commercially available as a wrapping film, was used as a supporting material. A single microhole was then created by simply manually punching through the film with a sharp needle. An ellipse shape was obtained due to the tip shape of the needle and the variation in the mechanical punching force. The major diameter of the ellipse was about 110 ± 10 μm and the minor diameter was about 15 ± 5 μm (Fig. 1(a)). The organic gel layer was prepared by dissolving PVC (3% m/m) in a solution of NPOE at 120 °C for 30 min including the supporting electrolyte, either 10 mM BTPPATPBCl or TBATPBCl, as well as ionophores. Ten microlitres of the PVC-NPOE mixture were then hot casted at 80 °C on the exit side of the microhole punched on the PVC supporting film and allowed to cool down for a minimum of 6 h to form the gel. From the FE-SEM data (see the ESI†), the PVC-NPOE gel was settled into the microhole structure without excessive flow on to the opposite surface of the supporting film.

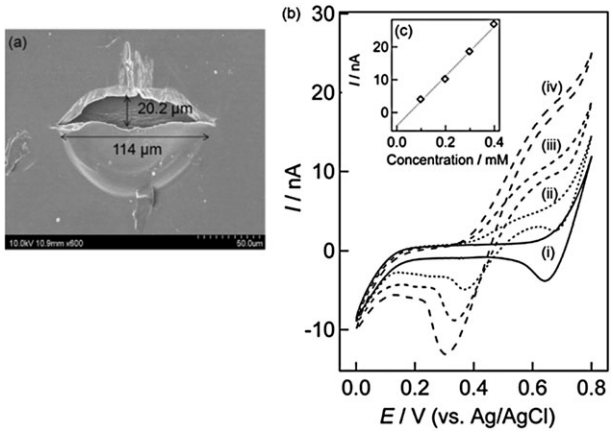

Fig. 1 (a) Field-emission scanning electron microscope (FE-SEM) image of a single ellipse-shaped microhole created in a commercially available food wrapping PVC film (12 μm thick). Diameters of longitudinal and transverse axes were 20 and 114 μm, respectively. (b) A series of cyclic voltammograms for different concentrations of TMA^+ ion transfer across the microhole interface between the aqueous and PVC-NPOE gel phases using Cell 1. (i) 10 mM LiCl in the absence of TMA^+ ion as well as (ii) 0.1 mM, (iii) 0.2 mM and (iv) 0.3 mM TMA^+ ion were used. Scan rate = 20 mV s^{-1}. (c) Plot of steady state currents *versus* TMA^+ ion concentrations. Dotted line shows a linear fit.

Electrochemical measurements

The electrochemical experiments were carried out using a computer-controlled potentiostat (Autolab PGSTAT30 Ecochemie). All the electrochemical data were acquired without IR drop compensation as well as being monitored by the General Purpose Electrochemical System (GPES) version 4.9 software package. Cyclic voltammetry and differential pulse stripping voltammetry were employed to characterize TMA^+ ion and proton transfer processes and further sensing capabilities.

III. Results and discussion

III.1 Ion transfer reactions across a single ellipse shaped microhole liquid/gel interface

The ion transfer behavior across a single ellipse shaped microhole interface between the aqueous and the PVC-NPOE gel phase was first characterized using cyclic voltammetry with the electrochemical cell set-up (Cell 1). As a model ion, TMA^+ ion transferring across the interface in middle of potential window set by Li^+ ion transfer at the positive potential and TBA^+ ion present in the organic phase at the negative potential.

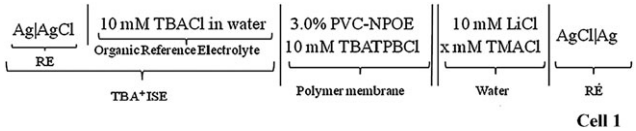

Fig. 1(b) shows a series of cyclic voltammograms obtained for the transfer of different concentrations of TMA^+ ions

from the aqueous phase to the organic phase (forward voltammetric sweep) in which a steady state response was observed due to the hemispherical diffusion on the aqueous side of the hole. A peak-shaped response was observed for the reverse sweep due to the linear diffusion by the egress ion transfer out of the microhole from the viscous organic phase to aqueous phase. An increase in the steady state current as the TMA^+ ion concentration increases with a linear slope of 77 nA mM^{-1} (see Fig. 1(c)). The observed current due to the ingress ion transfer can be regarded as a mass transport limited current to a micro-disc electrode case. However, our microhole interface is an ellipse like a microelliptic disk. The use of elliptical electrodes is seldom described in the literature,[22–24] but this type of electrode has several interesting electrochemical properties; for example, Wightman and coworkers have built elliptical carbon fiber microdisks in order to benefit from the reactivity of the edges of carbon microfibers.[23] The steady state current associated with an ionic species (i) transferring across an ellipse microhole interface can be described by eqn (1);[22]

$$I_{ss} = 2\pi n z_i FDca/K(\varepsilon) \quad (1)$$

where n is the number of hole, z_i is the charge of ionic species, F is the Faraday constant, D is the diffusion coefficient, c is the concentration of ionic species, $\varepsilon = \sqrt{\{1 - (b^2/a^2)\}}$ is the eccentricity, a and b are the semimajor and the semiminor axis of the ellipse, respectively, and $K(\varepsilon)$ is the complete elliptic integral of the first kind;

$$K(\varepsilon) = \int_0^{\pi/2} d\theta/\sqrt{1 - \varepsilon^2 \sin^2\theta} \quad (2)$$

For a limited value of ε, we can then simplify the eqn (1) as follows:

$$I_{ss} = 4 n z_i FDca[1 - 1/4\ \varepsilon^2 - 5/64\ \varepsilon^4] \quad (3)$$

The observed steady state current (3.89×10^{-9} A) was slightly larger than that of the calculated steady state current (2.48×10^{-9} A) using eqn (3). This may be due to a possible unevenness in edges and shape (ellipse) caused by the manual punching process and also a possible overflowing of the gel formed on the other side around the hole of which both phenomena could enlarge the size of interface. Another possibility is that this increase could be a result of the contribution of the edge effects to the enhancement of mass transport associated with TMA^+ ion transferring across the interface.[23] This phenomenon will further be studied by simulating the mass transport at elliptical microdisk electrochemical systems in a subsequent paper.

Further studies clarifying the peak shape of the ion transfer at reverse scan were performed by obtaining a series of cyclic voltammograms of 0.1 mM TMA^+ at different scan rates. It was observed that the reverse peak current increases proportionally as a function of the square root of scan rate with a linear slope of 24.39 nA $(V\ s^{-1})^{-1/2}$ (see Fig. 2) which is similar to the result reported for TMA^+ ion transferring back from the PVC-NPOE gel phases to the aqueous phase across an array of microhole interfaces.[5] This is mainly due to the dominant linear diffusion inside the microhole filled with the viscous organic phase occurred by the transfer of the ions back

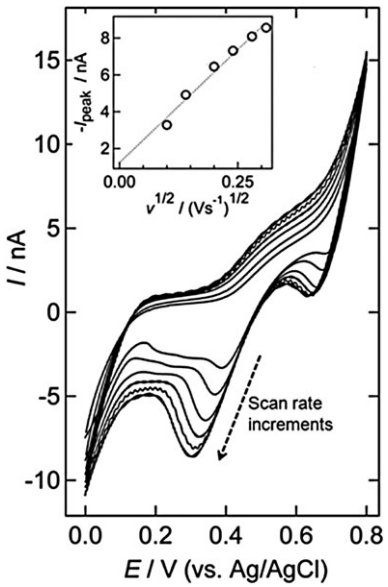

Fig. 2 Cyclic voltammograms for 0.1 mM TMA^+ ion transfer across the microhole interface between the aqueous and PVC-NPOE gel phases using Cell 1 at various scan rates ranging from 10, 20, 40, 60, 80 to 100 mV s^{-1}. Inset shows a plot of peak current associated with TMA^+ ion transferring back from the PVC-NPOE gel layer to the aqueous phase as a function of the square root of scan rates.

from the organic layer to the aqueous phase. Whereas the increment in the sweep rate did not effect on the forward peak current due to the hemispherical diffusion of ions governed by the ion transfer from the aqueous phase to the organic phase across the microhole interface. It must also be mentioned that the increase in the scan rate causes a small shift of the reverse scan peaks towards more negative potential because of uncompensated IR drop.

III.2 Assisted transfer of protons by ETH1778

The well-characterized ion transfer properties across the polarized microhole interface put us in a position to investigate proton sensing capabilities based on the assisted transfer of proton with the proton selective ionophore, octadecyl isonicotinate, commercially known as ETH1778 present in the PVC-NPOE gel layer. The ionophore containing nitrogen molecule in an aromatic ring offering three hydrogen acceptors has been used in polymeric ion selective electrode for pH sensing.[25–27] The assisted transfer of proton by ETH1778 were characterized using cyclic voltammetry and Cell 2.

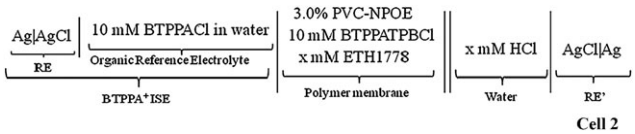

For the facilitated transfer of protons by ETH1778 across the ITIES, two different electrochemical responses can be observed depending upon the ratio of the concentration and diffusion coefficient of both the proton and the ligand. For the case of excess concentrations of ligand ($D_{H^+}[H^+] \ll D_L[L]$), the observed limiting current is proportional to the

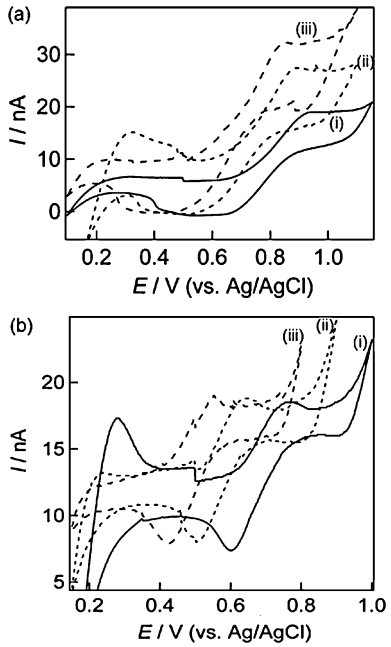

Fig. 3 Cyclic voltammograms for the assisted transfer reaction of protons by ETH1778 present in the PVC-NPOE gel layer using Cell 2. The concentration of HCl present in the aqueous phase was varied (a) from (i) 0.1 mM, (ii) 1 mM to (iii) 5 mM for 10 mM ETH1778 and (b) from (i) 10 mM, (ii) 50 mM to (iii) 100 mM for 1 mM ETH1778. 10 mM BTPPATPBCl was used as an organic supporting electrolyte and scan rate was 20 mV s^{-1}.

concentrations of the proton. Here it must be mentioned that the diffusion coefficient of the ligand in the PVC-NPOE phase is known to be over 10–100 times slower than that of proton in water (3.0×10^{-5} cm^2 s^{-1}).[28] Various concentration ratios were investigated to observe experimentally two different dominant cases. Cyclic voltammograms in Fig. 3(a) were obtained for $D_{H^+}[H^+] \ll D_L[L]$ by varying the proton concentrations from 0.1 to 5 mM while ETH1778 was fixed as 10 mM. The steady state currents occurred due to the assisted transfer of protons from the aqueous phase to the PVC-NPOE gel layer by ETH1778 increase linearly as a function of proton concentrations. On the other hand, for the case of excess concentration of protons ($D_L[L] \ll D_{H^+}[H^+]$, the limiting current is dominated by the concentration of the ligand. Cyclic voltammograms shown in Fig. 3(b) where the proton concentrations were in excess (10 to 100 mM) of the fixed concentration of the ionophore (1 mM), no rise of steady state currents were occurred while the shift in half-wave potential towards more negative potential was observed with the increase of proton concentrations.

In addition, the reversibility of the proton transfer was investigated using the plot of $\ln[(I_{ss} - I)/I]$ *versus* the applied potential. From the obtained linear curve with a slope equal to 30.3 mV was relatively in good agreement with the value of $RT/(zF)$ (25.7 mV) according to the eqn (4)[29] considering the uncompensated Ohmic drop and thus the ion transfer reaction can be regarded as reversible.

$$\Delta_o^w\phi - \Delta_o^w\phi_i^o = RT/zF \ln[D_i^w/D_i^o] - RT/zF \ln[(I_{ss} - I)/I] \quad (4)$$

where $\Delta_o^w\phi$ and $\Delta_o^w\phi_i^o$ represent the standard and formal ion transfer potential, respectively and D_i^w and D_i^o are the diffusion coefficients of the ion (i) in the aqueous and organic electrolyte phases, respectively.

Confirming the reversibility of the proton transfer, we could estimate the association constant in the case of the excess proton system shown in Fig. 3(b) using the eqn (5) derived for the reversible half wave potential for the ion transfer reaction across a microdisc interface;[28]

$$\Delta_o^w\phi_{1/2} = \Delta_o^w\phi^o + RT/F \ln(D_L/D_{LH^+}) - RT/zF \ln(\beta_1^o c_{H^+}) \quad (5)$$

where β_1^o is the association constant (normally expressed as log β_1^o), $\Delta o^w\phi_{1/2}$ and $\Delta o^w\phi^o$ are the half wave potential of assisted proton transfer by ETH1778 and formal transfer potential of proton across the water|NPOE respectively. c_{H^+} is the proton concentration and D_L and D_{LH^+} are the diffusion coefficients of the ligand and ligand–proton complex respectively. Assuming that the diffusion coefficient of the ligand is equal to that of the ligand–proton complex ($D_L = D_{LH^+}$),[30] the eqn (5) can be rewritten as:

$$\Delta_o^w \phi_{1/2} - \Delta_o^w \phi^o = -RT/zF \ln (\beta_1^o c_{H^+}) \quad (6)$$

By fitting the plot of $(\Delta_o^w\phi_{1/2} - \Delta_o^w\phi^o)$ *versus* ln c_{H^+} retreated from data in Fig. 3(b) using the eqn (6), the value of association constant (log β_1^o) of 10.8 was obtained. Here the value of the formal transfer potential of proton (458 mV) across the water|NPOE interface taken from the literature[31] was used, assuming that the formal transfer potential value of proton across the water|PVC-NPOE gel interface is similar to that of the water|NPOE interface.[28]

III.3 Glucose sensing with amperometric proton selective sensors

Scheme 1 shows a simplified detection scheme for the detection of glucose by means of measuring protons from gluconic acid produced during the enzymatic degradation of glucose by glucose oxidase. Briefly, the enzyme first oxidizes the aldehyde group on the C-1 of β-D-glucose to a carboxyl group resulting in the formation of glucono-δ-lactone which is further hydrolyzed to gluconic acid spontaneously.[32] The gluconic acid then produces protons in the aqueous phase which is proportionally increased as a function of the glucose concentration. The generated protons finally transfer across the microhole-ITIES facilitated by the proton selective ionophore, ETH1778 present in the organic phase. A similar sensing methodology has been previously reported when using an ionophore, 3-(2-pyridyl)-5, 6-diphenyl-1,2,4-triazine (PDT) for selectively binding to protons in aqueous phases.[19]

Fig. 4 shows a series of cyclic voltammograms for the sensing of protons generated from 6 and 18 mM of glucose with 10 nM glucose oxidase when using Cell 3. Here the concentration of enzyme was kept low to reduce any potential formation of bilayers at the interface for higher concentrations of the enzyme.[33] A steady-state behavior within the potential window on the forward sweep was observed for the assisted transfer of protons by ETH 1778 across the microhole-ITIES,

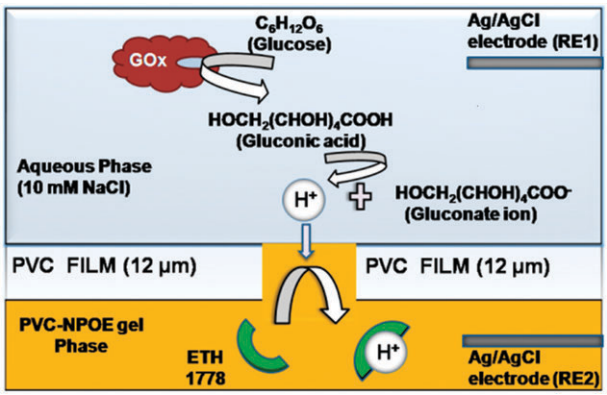

Scheme 1 A simplified schematic showing an amperometric glucose sensing methodology *via* measuring the current associated with the assisted transfer of protons across the microhole-ITIES by the proton selective ionophore. Glucose is oxidized by glucose oxidase to produce gluconic acid which releases protons in the aqueous phase. Protons then transfer across the microhole-ITIES assisted by ETH1778 present in the organic phase.

where protons were generated from glucose *via* the glucose oxidase reaction.

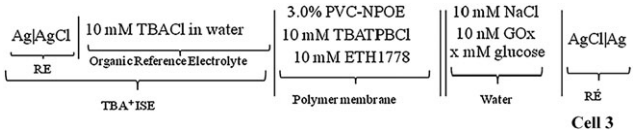

In order to improve the sensitivity and accuracy for the glucose sensing, differential pulse stripping voltammetry was applied with the preconditioning step at a potential of 0.3 V for 5 s. The preconcentration time was optimized at a pre-concentration potential of 0.6 V. Variation in the measured peak currents associated with proton transfer was observed depending upon deposition times and a deposition time of 20 s

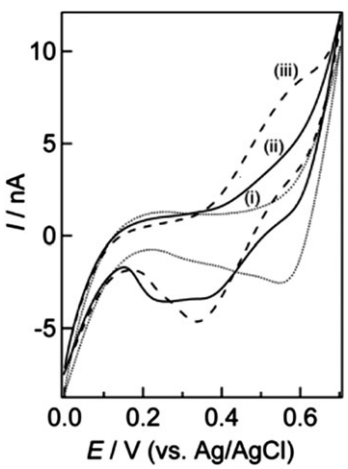

Fig. 4 Cyclic voltammograms obtained for the assisted transfer of protons from gluconic acid produced by the oxidation of different concentrations of glucose using 10 nM glucose oxidase. (i) 10 mM NaCl in the absence of glucose, (ii) 6 mM glucose and (iii) 18 mM glucose were used and Cell 3 was used with 10 mM TBATPBCl as an organic supporting electrolyte. Scan rate was 20 mV s^{-1}.

was selected as an optimum condition. Differential pulse stripping voltammograms were obtained for various concentrations of glucose ranging from 2 to 24 mM which is the general concentration range of glucose in human blood plasma. The measured peak current was proportionally increased as a function of glucose concentrations from 0 to 18 mM (see Fig. 5(a)). All measurements were taken without any further sample treatment such as stirring or agitation. An excellent linear fit over the glucose concentration range studied was also obtained by averaging the data points at each concentration of glucose from three different sets of microhole proton sensors and reasonable reproducibilities were achieved within the error of less than 10% (see Fig. 5(b)).

Finally, we have also tested the effects of major interfering ionic species, in particular electroactive species such as ascorbic acid and uric acid present in blood samples which is still challenging task for conventional glucose biosensors based on redox reactions of glucose by glucose oxidase with H_2O_2. When using our amperometric proton selective sensors negligible effects from both uric acid and ascorbic acid upto 0.3 mM on the measurements of glucose were observed, which is one of the greatest advantage of using the proton sensors.

IV. Conclusions

We have developed a cost effective amperometric ion selective sensor utilizing ion transfer reactions across a polarized single microhole interface between an aqueous and a PVC-NPOE gel phase. Well-characterized ion transfer reactions across the single microhole interface between the aqueous and the PVC-NPOE gel phases provided a good linear response for determining ion concentrations in the aqueous phase.

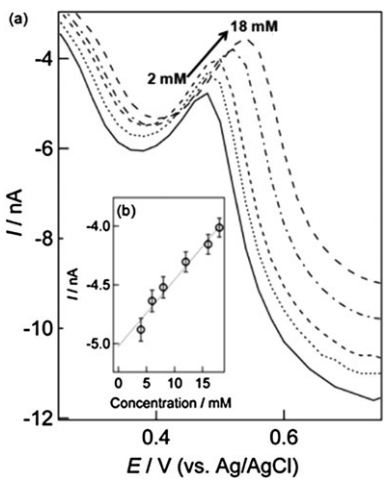

Fig. 5 (a) Differential pulse stripping voltammograms for various concentrations of H^+ ion transfer assisted by 10 mM ETH1778. The scan was directed from high to low potentials to drive H^+ ion transfer from the PVC-NPOE gel layer to the aqueous phase containing different concentrations of glucose (2, 6, 10, 14 and 18 mM) by applying deposition potential of 0.6 V for 20 s prior to analysis. The pulse conditions were as follows: potential increment = 20 mV, pulse potential = 50 mV, pulse duration = 50 ms and scan rate = 20 mV s^{-1}. (b) A plot of average peak current values for glucose sensing with respect to various concentrations of glucose using three different proton selective microhole-ITIES sensors.

In addition a proton selective sensor based on the facilitated ion transfer across the single microhole interface by the ETH1778 in the PVC-NPOE was developed and their electrochemical responses were thoroughly investigated for the sensing capabilities. The proton selective sensor with differential pulse stripping voltammetry was finally employed to measure glucose concentrations up to 18 mM, which is the common concentration range of the glucose in human blood plasma with a tolerance of common interfering species uric acid and ascorbic acid up to 0.3 mM. We envision that the cost-effective amperometric ion selective sensor based on facilitated ion transfer reactions can be employed for a wide spectrum of biological and environmental related research areas by tailoring target selective ionophores in the organic phase.

Acknowledgements

This work was supported by the New & Renewable Energy of the Korea Institute of Energy Technology Evaluation and Planning (KETEP) grant funded by the Korea government Ministry of Knowledge Economy (No. 20093020030020-11-1-000).

References

1 P. Jing, S. He, Z. Liang and Y. Shao, *Anal. Bioanal. Chem.*, 2006, **385**, 428–432.
2 F. Reymond, D. Fermín, H. J. Lee and H. H. Girault, *Electrochim. Acta*, 2000, **45**, 2647–2662.
3 D. W. M. Arrigan, *Anal. Lett.*, 2008, **41**, 3233–3252.
4 F. Silva, M. J. Sousa and C. M. Pereira, *Electrochim. Acta*, 1997, **42**, 3095–3103.
5 H. J. Lee, P. D. Beattie, B. J. Seddon, M. D. Osborne and H. H. Girault, *J. Electroanal. Chem.*, 1997, **440**, 73–82.
6 H. J. Lee, C. M. Pereira, A. F. Silva and H. H. Girault, *Anal. Chem.*, 2000, **72**, 5562–5566.
7 R. Zazpe, C. Hibert, J. O'Brien, Y. H. Lanyon and D. W. M. Arrigan, *Lab Chip*, 2007, **7**, 1732–1737.
8 N. Nishi, H. Murakami, S. Imakura and T. Kakiuchi, *Anal. Chem.*, 2006, **78**, 5805–5812.
9 J. Langmaier and Z. Samec, *Anal. Chem.*, 2009, **81**, 6382–6389.
10 M. Rimboud, C. Elleouet, F. Quentel, J.-M. Kerbaol and M. L'Her, *J. Electroanal. Chem.*, 2008, **622**, 233–237.
11 A. Benvidi, S. N. Lanjwani and Z. Ding, *J. Electroanal. Chem.*, 2010, **641**, 99–103.
12 Z. Samec, E. Samcová and H. H. Girault, *Talanta*, 2004, **63**, 21–32.
13 H. J. Lee, G. Lagger, C. M. Pereira, A. F. Silva and H. H. Girault, *Talanta*, 2009, **78**, 66–70.
14 M. D. Scanlon, G. Herzog and D. W. M. Arrigan, *Anal. Chem.*, 2008, **80**, 5743–5749.
15 M. D. Scanlon, E. Jennings and D. W. M. Arrigan, *Phys. Chem. Chem. Phys.*, 2009, **11**, 2272–2280.
16 P. J. Rodgers, P. Jing, Y. Kim and S. Amemiya, *J. Am. Chem. Soc.*, 2008, **130**, 7436–7442.
17 T. Osakai, T. Kakutani and M. Senda, *Anal. Sci.*, 1988, **4**, 529–530.
18 M. D. Osborne and H. H. Girault, *Mikrochim. Acta*, 1995, **117**, 175–185.
19 C. M. Pereira, J. M. Oliveira, R. M. Silva and F. Silva, *Anal. Chem.*, 2004, **76**, 5547–5551.
20 K. Holub, H. Jänchenová, K. Štulík and V. Mareček, *J. Electroanal. Chem.*, 2009, **632**, 8–13.
21 Z. Ding, D. J. Fermín, P. F. Brevet and H. H. Girault, *J. Electroanal. Chem.*, 1998, **458**, 139–148.
22 S. Bruckenstein and J. Janiszewska, *J. Electroanal. Chem.*, 2002, **538–539**, 3–12.
23 K. Pihel, Q. D. Walker and R. M. Wightman, *Anal. Chem.*, 1996, **68**, 2084–2089.
24 R. S. Kelly and R. M. Wightman, *Anal. Chim. Acta*, 1986, **187**, 79–87.
25 P. Bühlmann, E. Pretsch and E. Bakker, *Chem. Rev.*, 1998, **98**, 1593–1687.
26 P. Upreti, L. E. Metzger and P. Bühlmann, *Talanta*, 2004, **63**, 139–148.
27 X.-J. Liu, B. Peng, F. Liu and Y. Qin, *Sens. Actuators, B*, 2007, **125**, 656–663.
28 H. J. Lee, C. Beriet and H. H. Girault, *J. Electroanal. Chem.*, 1998, **453**, 211–219.
29 A. M. Bond, K. B. Oldham and C. G. Zoski, *J. Electroanal. Chem.*, 1988, **245**, 71–104.
30 H. Matsuda, Y. Yamada, K. Kanamori, Y. Kudo and Y. Takeda, *Bull. Chem. Soc. Jpn.*, 1991, **64**, 1497–1508.
31 S. M. Ulmeanu, H. Jensen, Z. Samec, G. Bouchard, P. Carrupt and H. H. Girault, *J. Electroanal. Chem.*, 2002, **530**, 10–15.
32 S. Ramachandran, P. Fontanille, A. Pandey and C. Larroche, *Food Technol. Biotechnol.*, 2006, **44**, 185–195.
33 D. G. Georganopoulou, D. E. Williams, C. M. Pereira, F. Silva, T. Su and J. R. Lu, *Langmuir*, 2003, **19**, 4977–4984.